Geothermics 89 (2021) 101992

Contents lists available at ScienceDirect

Geothermics

journal homepage: www.elsevier.com/locate/geothermics

Laboratory investigations of the physical parameters influencing the *in situ* leaching of tungsten

Máté Osvald [a,*], Andrew Kilpatrick [b], Christopher A. Rochelle [b], János Szanyi [a], Béla Raucsik [a], Tamás Medgyes [a], Balázs Kóbor [a]

[a] University of Szeged, Department of Mineralogy, Geochemistry and Petrology, Egyetem u. 2. Szeged, H-6722, Hungary
[b] British Geological Survey, Nicker Hill, Keyworth, Nottingham, NG12 5GG, United Kingdom

ARTICLE INFO

Keywords:
Geothermal
EGS
Tungsten
In situ leaching

ABSTRACT

Tungsten leaching potential from geothermal reservoirs was investigated using a flow-through reactor with the characteristic physical properties of a geothermal reservoir. Tungsten minerals were tested at 200 °C, 250 °C and 300 °C, and 0.5 and 1.0 mL/min flow rates to determine the most favourable conditions for the mobilisation of tungsten. *In situ* leaching yielded tungsten concentrations of 1–182 mg/L in the leachates, with pure scheelite being the most effective in mobilising tungsten. The highest concentrations, which were obtained at 300 °C, were generally observed in the first 30–60 min because of the rapid fluid–rock interactions in the geothermal reservoir.

1. Introduction

Contact time, which describes the fluid residence time in a geothermal reservoir, is an important physical property of an enhanced or engineered geothermal system (EGS). It is a complex factor that defines the behaviour of the potentially produced fluid, and it is influenced by many different physical and chemical processes. The contact time is highly dependent on the origin of the fluid in the reservoir and is therefore unique for each point in the reservoir. Residence time can be estimated *via* mass and heat transport calculations, fracture modelling, tracer tests and monitoring, and is generally 300–500 h in an average hydrothermal system (Huenges, 2010; Waber et al., 2017). The interactions between the fluid and reservoir may result in dissolution–precipitation processes during this residence time, especially if a fluid with a relatively low amount of total dissolved solids is pumped into an EGS *via* injection wells, thereby enriching the fluid by the time it is produced. This natural process can be controlled artificially and manipulated to dissolve favourable materials.

The idea of further harnessing brines has received considerable attention in enhancing the economics of geothermal energy utilisation, with lithium being the first mineral to be extracted from geothermal fluids. These lithium-producing operations have taken place in felsic magmatic environments in New Zealand (Kennedy, 1961; Mroczek et al., 2015) and various igneous sources, including granitoid environments, in the United States (Bourcier et al., 2005; Kesler et al., 2012; Neupane and Wendt, 2017). Such geological settings are optimal for establishing an EGS, with the co-production of metals alongside energy production presenting a feasible option in many cases (Németh et al., 2016; Kilpatrick et al., 2017; Szanyi et al., 2017). The proven viability of lithium production from geothermal brines serves as a good motivation to investigate the production potential of extracting other elements.

The European Commission (2017) reviewed the necessary raw materials for the techno-economic development of the European Union and identified those materials that yielded a substantial supply risk (*i.e.* high uncertainties in securing sustainable supply) while also assessing current reserves and resources. Tungsten was evaluated as the leading element in terms of economic importance, with the supply risk above the determined threshold. Tungsten is a metal with the highest melting point of all elements (except carbon), as well as the highest atomic weight and density of all metals, making it a widely used metal with numerous industrial, civilian and military applications. It is essential for many high-strength, high-temperature applications, such as wood and metalworking, mining, steel hand tools, wear protection, ammunition, studded tyres and chemical use (Amer, 2000; Luo et al., 2003; Bednar et al., 2008). It has also been designated as a 'critical material' and 'strategic resource' within the European Union (Linnen et al., 2012; EC, 2017).

Tungsten is commonly found as a mobile tungstate anion in the environment, which is able to create polymers with itself and other anions (Bednar et al., 2008). It is utilised from ore (0.3 %–1 % WO_3), ore

* Corresponding author.
E-mail address: osimate@gmail.com (M. Osvald).

https://doi.org/10.1016/j.geothermics.2020.101992
Received 14 November 2019; Received in revised form 6 October 2020; Accepted 18 October 2020
Available online 1 November 2020

Table 1
Most significant tungsten containing minerals (based on data from Sarin, 2014).

Mineral	Chemical name	Formula	WO_3 content (w %)
Ferberite	Iron tungstate	$FeWO_4$	76.3
Hübnerite	Manganese tungstate	$MnWO_4$	76.6
Stolzite	Lead tungstate	$PbWO_4$	50.9
Scheelite	Calcium tungstate	$CaWO_4$	80.6
Wolframite	Iron tungstate and manganese tungstate	$(Fe,Mn)WO_4$	76.3–76.6

concentrate (7 %–60 % WO_3) and scrap (40 %–95 % WO_3) and potentially *via* unconventional production, such as geothermal brines (Onozaki et al., 1976; Luo et al., 2003). Che et al. (2013) identified tungsten concentration ranges from 12 mg/L to much higher values in its natural (granitoid or pegmatiod) environments. They also found that rocks with high tungsten concentrations are often very rich in lithium as well. Therefore, ongoing lithium extraction from such environments provides a potential analogue for targeting tungsten production from similar environments.

China currently accounts for 82 % of the total global conventional extraction of tungsten, with the next closest producers being Vietnam (6 %), Russia (2 %) and Canada (2 %). Tungsten is mined throughout Europe, with mines in the United Kingdom, Austria, Portugal and Spain, but the supply is very limited, accounting for approximately 2.7 % of global production (Sverdrup et al., 2017; Tkaczyk et al., 2018). Tungsten demand is forecasted to grow by 5–8 % annually, which poses a potential problem if China cuts exports because of increased domestic demand (Pulidindi and Chakraborty, 2018). The main sources of tungsten production are wolframite ($(Fe,Mn)WO_4$, half of the total production), scheelite ($CaWO_4$, one-third of the total production), ferberite ($FeWO_4$) and hübnerite ($MnWO_4$) ores (Sverdrup et al., 2017). The tungsten content of each mineral is listed in Table 1. Although secondary sources of production are also utilised (approximately 4 % of the total production), recycling provides an abundant source (35 %–50 %) with potential for future growth (Sverdrup et al., 2017).

In this article the potential of tungsten mobilisation with deionised water was explored by performing high-temperature flow-through experiments. In the future, leaching experiments with different fluids will follow this work.

2. Experimental

2.1. Reagents and solid materials

All of the chemicals were of reagent grade or higher purity and used without further purification. The deionised (DI) water used in the experiments had a conductivity of 6.3 μS/m. Inert quartz sand (grain size of 0.1–0.8 mm) was purchased from Molar Chemicals (Hungary). Scheelite powder with 99+% purity was purchased from MaTecK GmbH (Germany), and ferberite concentrate was obtained from Panasqueira Mine (Portugal). The crystallinity of the applied scheelite standard was tested by routine XRPD measurement. According to the results it can be characterized by an average crystallite size of ~75–100 nm. The purity of the concentrate was determined as described below (Fig. 3).

Aqueous leaching of the stock tungsten yields dissolved tungsten concentrations that are controlled by the solubility of tungstate mineral phases (Bednar et al., 2009; Gürmen et al., 1999; Martins et al., 2007). Therefore, a dilution of the tungsten material was used in each leaching experiment, consisting of 8.00 g of tungsten mineral (scheelite and/or ferberite) mixed with inert quartz sand, which completely filled the 126 cm^3 volume of the reactor. A 10-min ultrasonic bath was then applied to the solid material mixture in the reactor to compress the mixture and minimise the pore size prior to the experiments.

2.2. High-pressure, high-temperature flow-through reactor setup

The leaching processes were investigated under continuous flow conditions using a flow-through reactor (Fig. 1). The reaction took place in a stainless steel high-performance liquid chromatography (HPLC)

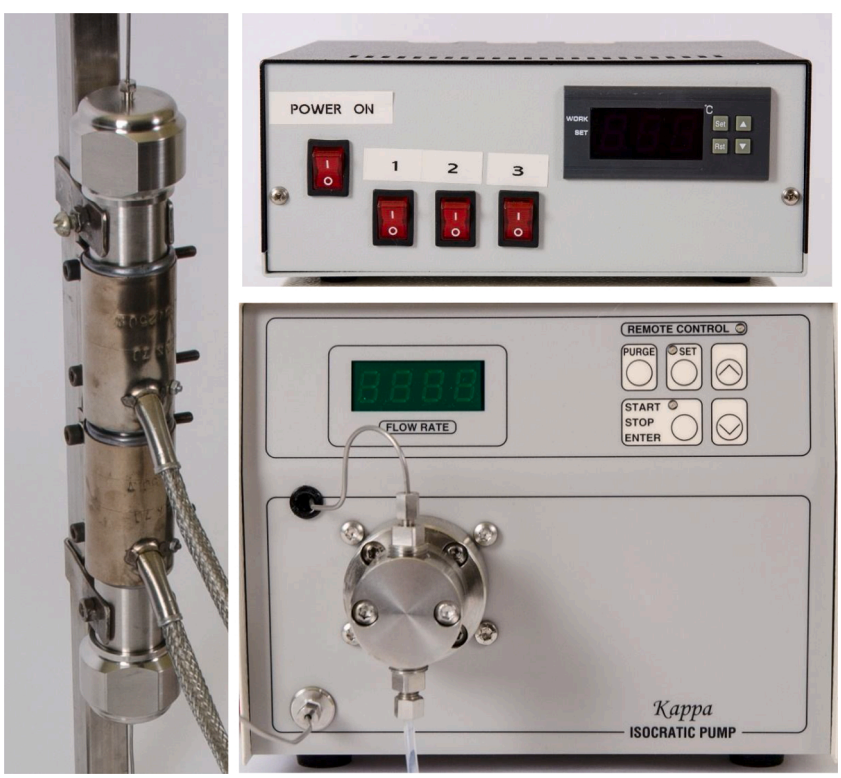

Fig. 1. Flow-through EHPV (left) and temperature control panel (upper right) of the HPLC pump (lower right) used in laboratory experiments.

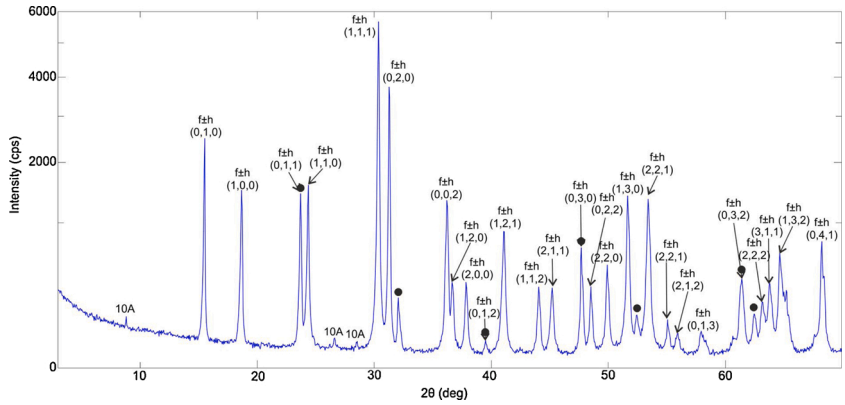

Fig. 2. XRPD pattern of the sample used in leaching experiments. Black dots indicate the most intensive reflections of ilmenite; Miller indices are listed in brackets. Abbreviations: 10A: 10 Ångström phase (probably muscovite); f ± h: ferberite ± hübnerite.

column that was 250 mm in length, with an inner diameter of 25.4 mm. The pressure in the column was maintained using an Ecom Kappa 10 Single-Plunger HPLC pump (Czech Republic). A 50-cm stainless steel capillary and a fluid back-pressure regulator were fitted at the outflow of the column. The length of this tubing helped to cool the outflowing fluid below 90 °C before being depressurised. Heating bands were attached to the HPLC column and controlled using a thermostat (WH-1435D proportional–integral–derivative controller digital thermostat with ±1 °C control regulation). This externally heated pressure vessel (EHPV) was loaded with an approximately 126 cm^3 sample and operated at a range of temperatures (200 °C, 250 °C and 300 °C) and a pressure of approximately 250 bar. These parameters correspond to depths of around 2.5–3 km in an average geothermal field (Massachusetts Institute of Technology (MIT, 2006; Breede et al., 2013). Two different flow rates (0.5 and 1.0 mL/min) were used in the reactor during the experiments, which resulted in a contact time of 30–100 min between the fluid and rock, allowing sufficient sample volumes to be collected for chemical analyses.

2.3. Sample collection and preparation

The samples did not undergo additional filtering prior to the analysis because stainless steel (316) frits with a nominal 2.0-μm pore size were placed at each end of the EHPV and effectively provided *in situ* filtering of the aqueous leachate samples. The collected samples did not undergo additional dilution because the concentrations were not high and a sufficient amount of sample could be produced with the above-mentioned continuous flow-through setup. The dissolved tungsten concentrations in the column leachates were determined as described below.

2.4. Instrumentation and analysis

The bulk mineralogical composition and characterisation of the ferberite concentrate was made *via* X-ray powder diffractometry (XRPD) using Rigaku Ultima IV diffractometer (Japan) with CuK_α radiation. The accelerating voltage was 50 kV at 40 mA, and the 2θ range was 3°–70°, operating at a scan speed of 1°/min and data acquisition steps of 0.05°. Bragg–Brentano geometry, graphite single crystal monochromator, proportional counter and divergence and detector slits (2/3°) were used during the XRPD analysis at the Department of Mineralogy, Geochemistry and Petrology, University of Szeged. A qualitative evaluation of the XRPD spectra was made using the ICDD (PDF2010) database of the Rigaku PDXL 1.8 software, and semiquantitative mineralogical composition was determined based on the reference intensity ratio method (Hubbard et al., 1976). Additionally, crystallinity of the scheelite standard was determined by the same software using Scherrer equation.

The tungsten concentrations were determined *via* inductively coupled plasma-optical emission spectrophotometry (ICP-OES) using a HORIBA Jobin Yvon ACTIVA-M spectrometer (France). The concentrations were determined using argon as both the coolant (16 L/min) and carrier (0.4 L/min) gas. The nebuliser pressure was 2.76 bar, and the wavelength was 207.912 nm. The instrument was calibrated using a blank and a series of four calibration standards (0, 1.0, 5.0 and 10.0 mg/L), each with a typical linear correlation coefficient (R^2) greater than 0.9999. The tungsten standard solution (1000 mg/L) was purchased from Merck (Germany).

All of the concentrations are reported in mg/L.

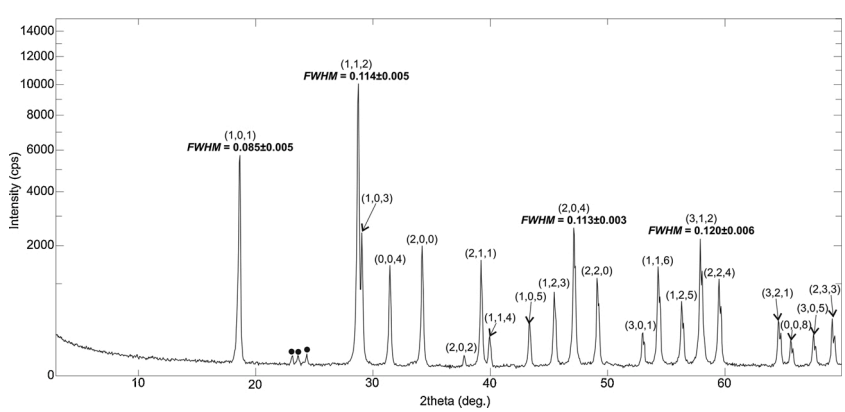

Fig. 3. XRPD pattern of scheelite reference material (CAS-Nr.: 7790-75-2) used for the experiments. Miller indices of scheelite are listed in brackets. Note that the sample contain almost pure scheelite with <1 m/m % krasnogorite (WO_3) as impurity (black dots). Full-width-at-half-maximum (FWHM) values of four selected intensive scheelite reflections are enhanced by bold characters.

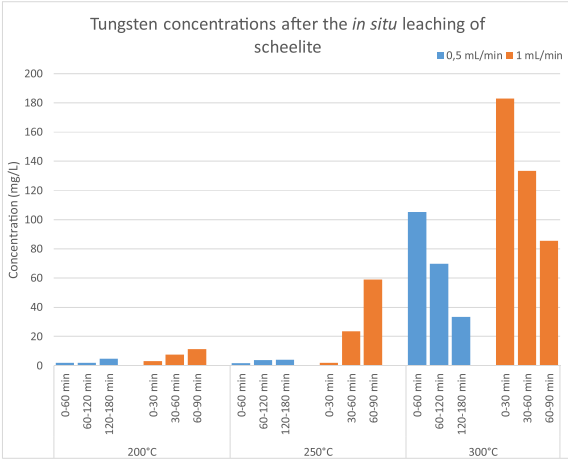

Fig. 4. Tungsten concentrations in the leachate after contacting scheelite with DI water under different geothermal reservoir scenarios.

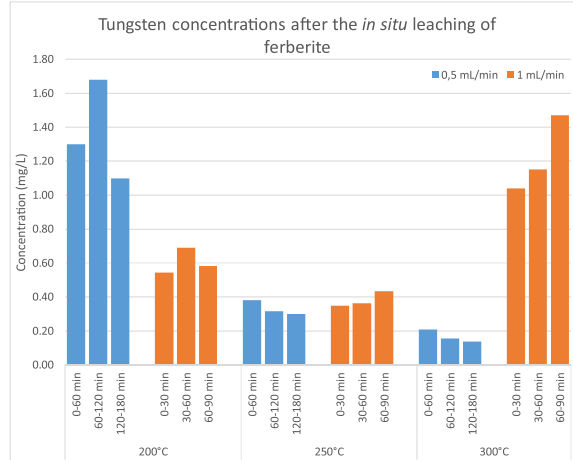

Fig. 5. Tungsten concentrations in the leachate after contacting ferberite with DI water under different geothermal reservoir scenarios.

3. Results and discussion

3.1. XRPD analysis of the solid samples

The analysed sample consists almost entirely of ferberite and hübnerite, with traces (1–2 m/m %) of a 10 Å layer silicate phase, which is most probably muscovite (Fig. 2). A trace amount (1– m/m^2 %) of ilmenite were also found in the sample. Quantification of the hübnerite and ferberite by XRPD method is rather problematic because they have almost identical structures and, as a consequence, their diffractometric profiles are very similar. The strongest reflection of the sample was detected at 2Θ = 30.358°, at an intermediate position between 30.45° and 29.84° which refer to 100 intensity (−1,1,1) reflections of pure ferberite and hübnerite endmembers of wolframite. This diagnostic reflection does not show a shoulder-like shape, but it can be characterized as a rather sharp peak with a full-width-at-half-maximum value of 0.162 ± 0.006°2Θ. Additionally, it has an asymmetry factor of 2.3 which suggests two overlapping reflections. Therefore, the sample is most likely composed of a mixture of both tungsten minerals, with a predominance of the ferberite. This conclusion is also confirmed by a small shoulder at 49.885°2Θ and a small intensity peak (15 cps) at 52.42°2Θ.

3.2. In situ leaching of scheelite with DI water eluent

The initial experiments were designed with pure tungsten minerals (scheelite or ferberite) and finally with a 1:1 mixture of scheelite and ferberite to isolate the effect of each mineral. The reactor was first filled with 8.0 g of scheelite (chemical grade) and inert quartz sand, which corresponds to a 5 % concentration of the 'active' material in the initial solid sample. Tungsten content of the solid $CaWO_4$ sample was 343 mg/kg.

The corresponding ICP-OES results from the scheelite leachates are shown in Fig. 3 and detailed properties of each experiment conducted with pure scheelite are listed in Table A1 appendix.

The main trend observed in the *in situ* leaching of scheelite is the effect of temperature on the dissolution rate, with increased tungsten release occurring as the temperature increased. The maximum concentrations at 200 °C were 5 and 11 mg/L at 0.5 and 1.0 mL/min flow rates, respectively. The 0.5 mL/min flow rate yielded approximately 4 mg/L, and the 1.0 mL/min flow rate yielded 60 mg/L at 250 °C. The concentration of the released tungsten increased with time, with the concentration at 250 °C and 1 mL/min increasing from 2 mg/L at 30 min to 60 mg/L at 90 min. The highest W concentrations were observed at 300 °C, ranging from 35 to 180 mg/L. However, it is important to note that tungsten concentration in the leachates decreased over time at this temperature. The reason for this decreasing trend could be that the mobility of scheelite is highest at 300 °C among the investigated temperatures, with the access to fresh fluid being the limiting factor in tungsten release. As soon as the fresh DI water contacted the 'active' material, it could rapidly dissolve as many ions as it could carry, such that its mobilisation rate declined over time.

3.3. In situ leaching of ferberite with DI water eluent

Given that both Fe^{2+} and Fe^{3+} ions are commonly found in natural environments, ferberite is chosen to determine if potential electron transfers would enhance tungsten mobilisation. The reactor was filled with 8.0 g of ferberite (concentrate from a tungsten mine) and inert quartz sand, which corresponds to a 5 % concentration of the 'active' material in the initial solid sample. Tungsten content of the solid $FeWO_4$ sample was 773 mg/kg.

The corresponding ICP-OES results from the ferberite leachates are shown in Fig. 4 and detailed properties of each experiment conducted with ferberite are listed in Table A2, appendix.

There is no distinct trend in the leaching of ferberite among the different geothermal reservoir scenarios, with *in situ* leaching yielding concentrations between 0.1 and 1.5 mg/L. The highest concentrations were reached at 200 °C and a 0.5 mL/min flow rate (>1 mg/L), whereas mobilisation was ineffective for the same flow rate at 250 °C (0.3–0.4 mg/l) and 300 °C (0.1–0.2 mg/L). Mobilisation was more effective at these temperatures and a 1.0 mL/min flow rate, yielding 0.3–0.5 mg/L concentrations at 250 °C and >1 mg/L concentrations at 300 °C. The difference between the highest and lowest concentrations in each scenario was negligible, and neither the temperatures nor the flow rates exhibited a notable influence on the mobility of ferberite, such that the leaching could be considered constant (low) throughout the experiments.

3.4. In situ leaching of the 1:1 ratio mixture of scheelite and ferberite with DI water eluent

A relatively mobile mineral, scheelite, was mixed with an immobile mineral, ferberite, which could potentially increase the rate of leaching by providing a Fe^{2+}/Fe^{3+} buffer *via* the potential changes of Fe in ferberite. The reactor was filled with 4.0 g of scheelite, 4.0 g of ferberite and inert quartz sand, which corresponds to a 5 % concentration of the 'active' material in the initial solid sample. Tungsten content of the solid mixture sample was 337 mg/kg.

The corresponding ICP-OES results from the conducted experiments

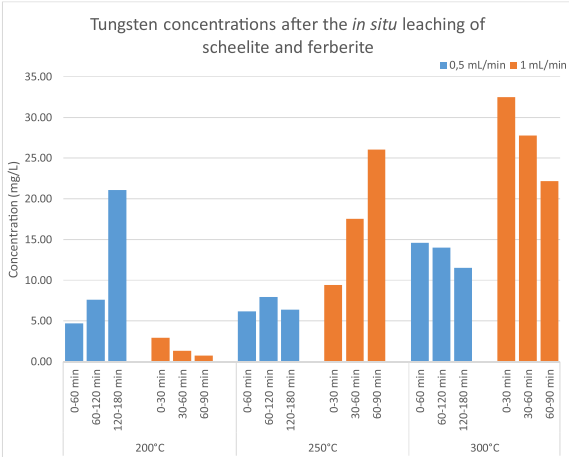

Fig. 6. Tungsten concentrations in the leachate after contacting the scheelite–ferberite mixture with DI water under different geothermal reservoir scenarios.

are plotted on Fig. 5 and details of each conducted experiment with a 1:1 mixture of scheelite and ferberite are listed in Table A3, appendix.

The mixture of relatively mobile (scheelite) and immobile (ferberite) tungsten minerals yielded minimum and maximum concentrations of 0.7 and 32.5 mg/L among the different geothermal reservoir scenarios. This concentration range was lower than that of the pure scheelite experiments and higher than that of the pure ferberite experiments. The higher flow rate could enhance the mobilisation as the tungsten concentrations increased from 8 to 26 mg/L at 250 °C and from 15 to 32 mg/L at 300 °C when the flow rate increased from 0.5 to 1.0 mL/min, respectively. This indicates that the rate-limiting step in the experiments is still the kinetic dissolution of scheelite, with most of the accessible scheelite molecules being rapidly mobilised by DI water, whereas the ferberite molecules remain immobile and do not facilitate tungsten release, therefore leading to lower tungsten concentrations in the mixtures (Fig. 6).

3.5. Thermodynamic approach for data interpretation

Solubility of solid materials are dependent on many different parameters; the direction of a solution/precipitation process is defined by thermodynamics. As it is discussed by Wood and Samson (2000), thermodynamic information of tungsten solubility is limited, especially in case of higher temperatures. Therefore, existing information at 25 °C could be utilised only, despite the absolute value is not the same as at high temperatures. However, trends and the direction of main reactions are the same, based on (Garrels and Christ, 1965).

In a chemical reaction, Gibbs standard free energy as a function of temperature determines the maximum amount of work that can be extracted from a thermodynamically closed system. If Gibbs energy of a solid material is a negative value, in our case it means that it has affinity to go into solution at a given temperature. If there are two solids with different Gibbs energy values, the material with more negative value will go into solution first and as the entropy changes, solution of the solid with less negative value will happen. Based on different experimental and literature data, Shen et al. (2018) compared thermodynamic data of major tungsten minerals and defined standard Gibbs free energy of formation as −1528.43 kJ/mol for $CaWO_4$ and −1053.91 kJ/mol for $FeWO_4$ at 25 °C temperature. This means that at 25 °C, $CaWO_4$ has the priority to go into solution, and when the source is depleted, $FeWO_4$ will follow. Thermodynamic data on $FeWO_4$ suggest that it is difficult to mobilise tungsten from ferberite.

The same trend appeared during the continuous leaching of scheelite and ferberite; when DI water was pumped through the 1:1 mixture of scheelite:ferberite, the concentration of tungsten in the fluid samples indicate that most of the scheelite was dissolved during the experiment and ferberite contributed to only a very small amount of tungsten. The challenge is to mobilise both materials, as in a natural (geothermal) environment, it is very likely that tungsten minerals will be in a mixed form. Therefore, understanding the solubility of a two-component mixture of solids with different properties is an important task, so artificial physical properties (fluid composition and residence time) could be tailored to the composition of the underground formation to approach effective metal mobilisation in the future.

Scaling in the reactor and in the capillary was not experienced during and after the leaching tests. A formation of secondary minerals could passivate the original scheelite surface and therefore reduce its reactivity, which can lead to a decrease in dissolution rate. Despite its importance, secondary W phases were not investigated within the framework of this article. As it could also happen naturally in a geothermal reservoir, the interest of this article is in the leached amount of tungsten regardless the changes in the initial solid sample.

Results in this paper suggest that if the reservoir has a temperature around 250 °C, residence time must be prolonged, as the efficiency of leaching at this temperature showed an increasing trend. In case of a reservoir with temperature around 300 °C, solubility of scheelite is extremely quick, and therefore subsurface enrichment of scheelite needs little time to go into solution. These observations are based on solely the results of the leaching tests. To fully understand a such system in the future, geochemical modelling is required. Therefore, the rapid increase in tungsten content at 300 °C might only mean that under these circumstances the reaction is rapid, however this does not indicate a thermodynamic equilibrium. It is possible, that lower temperatures could also mobilise this amount of tungsten, but in the laboratory, time was not enough to do so. As solid samples were ground, the surface area was increased notably, but equilibrium was still not reached during the laboratory tests.

4. Conclusions

Here, a continuous flow-through EHPV was used to study fluid–rock interactions under various geothermal reservoir conditions and investigate the potential of tungsten leaching and mobilisation in an EGS. Different tungsten minerals (scheelite and ferberite) were contacted with DI water at 200 °C, 250 °C and 300 °C under 250–280 bar pressure and different flow rates. Scheelite was much more mobile under the tested experimental conditions than ferberite. The experiments at 300 °C and a flow rate of 1 mL/min yielded tungsten concentrations of up to 180 mg/L in the leachate from pure scheelite, whereas concentrations of only 1–2 mg/L were obtained in the leachate from pure ferberite.

The effects of different physical parameters that could influence mild leaching were tested and compared, with the leaching time and temperature yielding significant differences in the tungsten concentrations during the leaching experiments. However, we noted that the influence of pressure on tungsten mobilisation could not be analytically investigated with the current experimental setup because of the pressure fluctuation in the single-plunger pump within a given time interval.

Time is an important parameter during the *in situ* leaching of tungsten with DI water. Although it seems intuitive that a longer leaching time would result in a higher mobilisation rate, this is not always the case. The dissolution of tungsten from pure scheelite reached equilibrium rapidly (usually in the first 30 min), with the longer experiments yielding lower concentrations over time. This trend becomes more obvious at higher temperatures, and the experiments at lower temperatures yielded low concentrations, regardless of leaching time. Nevertheless, pure scheelite yielded the highest concentrations compared to pure ferberite and scheelite–ferberite (1:1) mixture. Pure ferberite exhibited a much different trend, as it was much harder to mobilise, and the concentrations were much lower. Although the mobilisation rate was lower in the first hour of the flow-through leaching compared to

that in the second hour, the increase in mobilised material was only a few mg/L. The scheelite trend was more dominant in the experiments with the scheelite–ferberite (1:1) mixture, but ferberite was still difficult to mobilise in the mixture.

These experiments indicate that temperature has the largest influence on the *in situ* leaching of tungsten. The higher temperature (300 °C) experiments resulted in much more effective dissolution and mobilisation than the lower temperature (200 °C) experiments. Higher temperatures were not considered as the currently used 200 °C–300 °C temperature range represents the vast majority of high-enthalpy geothermal reservoirs.

The influence of the solid particle grain size on leaching was not investigated, with a uniform grain size used in the experiments for a better comparison among the experiments. This grain size, which was based on previous studies, was chosen to speed up the reaction time by increasing the contact surface for fluid–rock reactions. We note that this may not represent the actual contact surface, -volume or -time of a geothermal reservoir so that future studies should explore the effect of grain size on tungsten mobilisation. Future studies should also investigate the effect of different leaching fluids in the flow-through reactor under the same physical properties and experimental conditions, as well as different tungsten mineral compositions, to further constrain those parameters that effect tungsten mobilisation in geothermal settings.

Author statement

The authors do not wish to make any additional statement.

Data availability

The ICP-OES and XRPD data used to support the findings in this study are included within the article and appendices.

Declaration of Competing Interest

The authors reported no declarations of interest.

Acknowledgements

The authors would like to express their gratitude to Daniel Oliveira for providing the ferberite sample and Ferenc Szabó for the photographs of the laboratory equipment. Máté Osvald wish to acknowledge the support of NTP-NFTÖ-19-B-0014.

Appendix A

Table A1
Physical properties and results of the flow-through leaching experiments with scheelite.

Number	Temperature (°C)	Flow rate (mL/min)	Pressure (bar)	Material	Material amount (g)	Leachate volume (mL)	Analysis result (mg/L)
#1.1	200	1	220–250	$CaWO_4$	8	30	3.14 ± 0.02
#1.2	200	1	220–265	$CaWO_4$	8	30	7.51 ± 0.02
#1.3	200	1	220–250	$CaWO_4$	8	30	11.3 ± 0.1
#2.1	250	1	238–300	$CaWO_4$	8	29	2.03 ± 0.01
#2.2	250	1	250–270	$CaWO_4$	8	30	23.6 ± 0.2
#2.3	250	1	220–250	$CaWO_4$	8	30	58.8 ± 0.3
#3.1	300	1	186–250	$CaWO_4$	8	30	182.9 ± 0.7
#3.2	300	1	243–270	$CaWO_4$	8	30	133.4 ± 0.0
#3.3	300	1	218–250	$CaWO_4$	8	30	85.5 ± 0.4
#4.1	200	0.5	220–260	$CaWO_4$	8	32	1.87 ± 0.03
#4.2	200	0.5	220–260	$CaWO_4$	8	30	1.89 ± 0.02
#4.3	200	0.5	220–260	$CaWO_4$	8	30	4.84 ± 0.01
#5.1	250	0.5	240–250	$CaWO_4$	8	30	1.62 ± 0.00
#5.2	250	0.5	220–250	$CaWO_4$	8	30	3.69 ± 0.02
#5.3	250	0.5	220–250	$CaWO_4$	8	28	4.01 ± 0.02
#6.1	300	0.5	200–250	$CaWO_4$	8	29	105.3 ± 0.7
#6.2	300	0.5	195–250	$CaWO_4$	8	31	69.59 ± 0.39
#6.3	300	0.5	220–250	$CaWO_4$	8	30	33.35 ± 0.09

Table A2
Physical properties and results of the flow-through leaching experiments with ferberite.

Number	Temperature (°C)	Flow rate (mL/min)	Pressure (bar)	Material	Material amount (g)	Leachate volume (mL)	Analysis result (mg/L)
#7.1	200	1	220–274	$FeWO_4$	8	31	0.544 ± 0.001
#7.2	200	1	220–250	$FeWO_4$	8	30	0.69 ± 0.02
#7.3	200	1	220–250	$FeWO_4$	8	30	0.582 ± 0.005
#8.1	250	1	220–260	$FeWO_4$	8	30	0.348 ± 0.005
#8.2	250	1	250–270	$FeWO_4$	8	30	0.364 ± 0.004
#8.3	250	1	193–250	$FeWO_4$	8	30	0.435 ± 0.001
#9.1	300	1	220–258	$FeWO_4$	8	30	1.04 ± 0.00
#9.2	300	1	200–250	$FeWO_4$	8	30	1.15 ± 0.01
#9.3	300	1	206–235	$FeWO_4$	8	30	1.47 ± 0.01
#10.1	200	0.5	221–245	$FeWO_4$	8	30	1.30 ± 0.01
#10.2	200	0.5	220–237	$FeWO_4$	8	30	1.68 ± 0.01
#10.3	200	0.5	220–250	$FeWO_4$	8	30	1.10 ± 0.00
#11.1	250	0.5	220–251	$FeWO_4$	8	30	0.381 ± 0.02
#11.2	250	0.5	220–265	$FeWO_4$	8	30	0.316 ± 0.001
#11.3	250	0.5	220–250	$FeWO_4$	8	30	0.300 ± 0.003
#12.1	300	0.5	220–262	$FeWO_4$	8	30	0.210 ± 0.004
#12.2	300	0.5	205–250	$FeWO_4$	8	30	0.155 ± 0.000
#12.3	300	0.5	220–250	$FeWO_4$	8	30	0.136 ± 0.003

Table A3
Physical properties and results of the flow-through leaching experiments with a 1:1 mixture of scheelite and ferberite.

Number	Temperature (°C)	Flow rate (mL/min)	Pressure (bar)	Materials	Material amounts (g)	Leachate volume (mL)	Analysis result (mg/L)
#13.1	200	1	252–255	$CaWO_4 + FeWO_4$	4 + 4	29	2.90 ± 0.001
#13.2	200	1	230–272	$CaWO_4 + FeWO_4$	4 + 4	30	1.35 ± 0.01
#13.3	200	1	220–250	$CaWO_4 + FeWO_4$	4 + 4	30	0.736 ± 0.005
#14.1	250	1	237–250	$CaWO_4 + FeWO_4$	4 + 4	30	9.39 ± 0.37
#14.2	250	1	204–265	$CaWO_4 + FeWO_4$	4 + 4	29.5	17.53 ± 0.07
#14.3	250	1	213–250	$CaWO_4 + FeWO_4$	4 + 4	30	26.02 ± 0.10
#15.1	300	1	219–250	$CaWO_4 + FeWO_4$	4 + 4	30	32.48 ± 0.34
#15.2	300	1	245–254	$CaWO_4 + FeWO_4$	4 + 4	29.5	27.78 ± 0.18
#15.3	300	1	229–261	$CaWO_4 + FeWO_4$	4 + 4	30	22.167 ± 0.08
#16.1	200	0.5	226–245	$CaWO_4 + FeWO_4$	4 + 4	29.5	4.68 ± 0.03
#16.2	200	0.5	228–246	$CaWO_4 + FeWO_4$	4 + 4	30	7.60 ± 0.09
#16.3	200	0.5	245–263	$CaWO_4 + FeWO_4$	4 + 4	30	21.08 ± 0.09
#17.1	250	0.5	184–250	$CaWO_4 + FeWO_4$	4 + 4	30	6.18 ± 0.03
#17.2	250	0.5	207–250	$CaWO_4 + FeWO_4$	4 + 4	29.5	7.93 ± 0.77
#17.3	250	0.5	235–251	$CaWO_4 + FeWO_4$	4 + 4	29.5	6.41 ± 0.05
#18.1	300	0.5	221–250	$CaWO_4 + FeWO_4$	4 + 4	29.5	14.60 ± 0.0
#18.2	300	0.5	220–250	$CaWO_4 + FeWO_4$	4 + 4	29.5	14.00 ± 0.1
#18.3	300	0.5	259–268	$CaWO_4 + FeWO_4$	4 + 4	29.5	11.50 ± 0.0

Appendix B. Supplementary data

Supplementary material related to this article can be found, in the online version, at doi:https://doi.org/10.1016/j.geothermics.2020.101992.

References

Amer, A.M., 2000. Investigation of the direct hydrometallurgical processing of mechanically activated low-grade wolframite concentrate. Hydrometallurgy 58 (3), 251–259. https://doi.org/10.1016/S0304-386X(00)00134-1.

Bednar, A.J., Jones, W.T., Boyd, R.E., Ringelberg, D.B., Larson, S.L., 2008. Geochemical parameters influencing tungsten mobility in soils. J. Environ. Qual. 37 (1), 229–233. https://doi.org/10.2134/jeq2007.0305.

Bednar, A.J., Boyd, R.E., Jones, W.T., McGrath, C.J., Johnson, D.R., Chappell, M.A., Ringelberg, D.B., 2009. Investigations of tungsten mobility in soil using column tests. Chemosphere 75 (8), 1049–1056. https://doi.org/10.1016/j.chemosphere.2009.01.039.

Bourcier, W.L., Lin, M., Nix, G., 2005. In: Recovery of Minerals and Metals from Geothermal Fluids. 2003 SME Annual Meeting, Cincinnati, OH, United States. Lawrence Livermore National Laboratory. Feb 24 - Feb 26, 2003.

Breede, K., Dzebisashvili, K., Liu, X., Falcone, G., 2013. A systematic review of enhanced (or engineered) geothermal systems: past, present and future. Geotherm. Energy 1 (4), 27. https://doi.org/10.1186/2195-9706-1-4.

Che, X.D., Linnen, R.L., Wang, R.C., Aseri, A., Thibault, Y., 2013. Tungsten solubility in evolved granitic melts: an evaluation of magmatic wolframite. Geochim. Cosmochim. Acta 106 (1), 84–98. https://doi.org/10.1016/j.gca.2012.12.007.

European Commission, 2017. Directorate-General for Internal Market, Industry, Entrepreneurship and SMEs; Deloitte Sustainability; British Geological Survey; Bureau De Recherches Géologiques Et Minières; Netherlands Organisation for Applied Scientific Research. Study on the review of the list of Critical Raw Materials: Critical Raw Materials Factsheets. https://doi.org/10.2873/398823. ISBN: 978-92-79-72119-9.

Garrels, R.M., Christ, C.L., 1965. Solutions, Minerals, and Equilibria. Harper & Row, New York, p. 450.

Gürmen, S., Tımur, S., Arslan, C., Duman, I., 1999. Acidic leaching of scheelite concentrate and production of hetero-poly-tungstate salt. Hydrometallurgy 51 (2), 227–238. https://doi.org/10.1016/S0304-386X(98)00080-2.

Hubbard, C.R., Evans, E.H., Smith, D.K., 1976. The reference intensity ratio, I/I_c, for computer simulated powder patterns. J. Appl. Crystallogr. 9 (1), 169–174. https://doi.org/10.1107/S0021889876010807.

Huenges, E., 2010. Geothermal Energy Systems: Exploration, Development, and Utilization. WILEY-VCH. ISBN: 978-40833-527-40831-40833.

Kennedy, M., 1961. The recovery of lithium and other minerals from geothermal water at wairakei. In: Proceedings of United Nations Conference on New Sources of Energy, 1961. United Nations, New York.

Kesler, S.E., Gruber, P.W., Medina, P.A., Keoleian, G.A., Everson, M.P., Wallington, T.J., 2012. Global lithium resources: relative importance of pegmatite, brine and other deposits. Ore Geol. Rev. 48 (1), 55–69. https://doi.org/10.1016/j.oregeorev.2012.05.006.

Kilpatrick, A., Rochelle, C., Rushton, J., Lacinska, A., Fűzéri, D., Chenery, S., Marriot, A., Hamilton, E., Watts, M., Mountney, I., Kemp, S., 2017. Report on Metal Content Mobilisation Using Mild Leaching, CHPM2030 Deliverable D2.2, p. 374. https://doi.org/10.5281/zenodo.1207069.

Linnen, R.L., Lichtervelde, M.V., Černý, P., 2012. Granitic pegmatites as sources of strategic metals. Elements 8 (4), 275–280. https://doi.org/10.2113/gselements.8.4.275.

Luo, L., Miyazakia, T., Shibayama, A., Yen, W., Fujita, T., 2003. A novel process for recovery of tungsten and vanadium from a leach solution of tungsten alloy scrap. Miner. Eng. 16 (7), 665–670. https://doi.org/10.1016/S0892-6875(03)00103-1.

Martins, J.I., Lima, J.L.F.C., Moreira, A., Costa, S.C., 2007. Tungsten recovery from alkaline leach solutions as synthetic scheelite. Hydrometallurgy 85 (2–4), 110–115. https://doi.org/10.1016/j.hydromet.2006.08.007.

Massachusetts Institute of Technology (MIT), 2006. The Future of Geothermal Energy–Impact of Enhanced Geothermal System (EGS) on the United States in the 21st Century. Idaho National Laboratory, Idaho Falls, Idaho, p. 83415. ISBN: 0-615-13438-6.

Mroczek, E., Dedual, G., Graham, D., Bacon, L., 2015. Lithium extraction from wairakei geothermal fluid using electrodialysis. In: Proceedings World Geothermal Congress 2015. Melbourne, Australia, 19-25 April 2015.

Németh, N., Földessy, J., Hartai, É., Mádai, F., Kristály, F., Móricz, F., Debreczeni, Á., Kiss, A., Osvald, M., Szanyi, J., 2016. EGS-relevant Review of Orebody Structures: CHPM2030 Deliverable D1.3, p. 59. https://doi.org/10.5281/zenodo.581018.

Neupane, G., Wendt, D.S., 2017. In: Stanford, CaliforniaAssessment of Mineral Resources in Geothermal Brines in the US. 42nd Workshop on Geothermal Reservoir Engineering Stanford University, 13-15, p. 2017. February.

Onozaki, S., Nemoto, S., Hazeyama, T. (1976): Process for recovering tungsten from alkaline leaching solution of tungsten ores. United States Patent 3969484.

Pulidindi, K., Chakraborty, S., 2018. Tungsten Market Size by Application, by End-use, Industry Analysis Report, Regional Outlook, Application Growth Potential, Price Trends, Competitive Market Share & Forecast, 2018–2025.

Sarin, V.K., 2014. Comprehensive Hard Materials. Elsevier. ISBN: 978-0-08-096528-4.

Shen, L., Li, X., Taskinen, P., et al., 2018. Thermodynamics of tungsten ores decomposition process options. The minerals, metals & materials society 2018. Extraction 2018. In: Davis, B. (Ed.), The Minerals, Metals & Materials Series, pp. 2441–2453. https://doi.org/10.1007/978-3-319-95022-8_206.

Sverdrup, H.U., Olafsdottir, A.H., Ragnarsdottir, K.V., 2017. Modelling global wolfram mining, secondary extraction, supply, stocks-in-society, recycling, market price and resources, using the WORLD6 system dynamics model. Biophys. Econ. Resour. Qual. 2 (11), 17. https://doi.org/10.1007/s41247-017-0028-x.

Szanyi, J., Osvald, M., Medgyes, T., Kóbor, B.M., Tóth, T., Madarász, T., Kolencsikné Tóth, A., Debreczeni, Á., Kovács, B., Vásárhelyi, B., Rozgonyi-Boissinot, N., 2017. Recommendations for Integrated Reservoir Management: CHPM2030 Deliverable D2.1, p. 119. https://doi.org/10.5281/zenodo.1204833.

Tkaczyk, A.H., Bartl, A., Amato, A., Lapkovskis, V., Petrániková, M., 2018. Sustainability evaluation of essential critical raw materials: cobalt, niobium, tungsten and rare earth elements. J. Phys. D Appl. Phys. 51 (20), 27. https://doi.org/10.1088/1361-6463/aaba99.

Waber, H.N., Schneeberger, R., Mäder, U.K., Wanner, C., 2017. Constraints on evolution and residence time of geothermal water in granitic rocks at Grimsel (Switzerland). Procedia Earth Planet. Sci. 17 (1), 774–777. https://doi.org/10.1016/j.proeps.2017.01.026.

Wood, S.A., Samson, I.A., 2000. The hydrothermal geochemistry of tungsten in granitoid environments: I. Relative solubilities of ferberite and scheelite as a function of T, P, pH, and mNaCl. Econ. Geol. 95 (1), 143–182. https://doi.org/10.2113/gsecongeo.95.1.143.